

## Separation of Geometric Spreading, Scattering and Intrinsic Attenuation in VSP data

Amin Baharvand Ahmadi \* and Igor Morozov, University of Saskatchewan, Saskatoon, Saskatchewan, Canada  
amin.baharvand@usask.ca

### Summary

A model of fine-layer seismic scattering is derived from a well log located in a VSP area in Weyburn oilfield in Saskatchewan. This model is used to separate the effects of geometric spreading, scattering, and intrinsic attenuation (internal friction) recently measured from this VSP. The results show that above ~430-m depth, the geometric spreading and internal friction are primarily responsible for the observed amplitude decay. Below this level, scattering becomes comparable to internal friction, and from ~930 to 1160 m, scattering dominates the attenuation.

### Introduction

Attenuation of seismic-wave amplitudes is a complex phenomenon which is important to understand for many practical applications. In our recent study (Baharvand Ahmadi and Morozov, 2012) we used first-arrival amplitudes from a multi-offset VSP dataset to derive a layered anisotropic model for the attenuating properties of the subsurface. The model was based on inverting for the frequency-independent ( $\gamma$ ) and frequency-dependent ( $\kappa$ ) parts of the attenuation coefficient (Morozov, 2008):

$$\chi(f) = \gamma + \kappa f, \quad (1)$$

where  $f$  is the wave frequency. Parameter  $\gamma$  was associated with variations of geometric spreading (wavefront curvature; GS) and scattering, and  $\kappa$  was interpreted as caused by scattering and intrinsic attenuation (internal friction) of the medium. An intriguing problem is therefore whether the three factors of attenuation: GS, scattering, and internal friction can be separated. Here, we attempt such separation by modeling the effect of scattering in a finely layered reflection sequence.

Scattering is elastic attenuation, which means that it reduces the amplitudes of seismic arrivals while keeping the total energy of the wavefield constant (Shearer, 1999). Many studies attempted to separate scattering and anelastic attenuation by using different theoretical approaches and types of waves. Among them, note Dainty's (1981) model for S-waves within the lithosphere, which is the most similar to eq. (1) above, the energy-flux model by Frankel and Wennerberg (1987), and the seismic coda measurements by Mayeda et al. (1991). Our method below is close to the numerical model of scattering  $Q^{-1}$  by Richards and Menke (1983). Using a well log from the same area in which the attenuation model (1) was derived, we simulate the transmitted energy flux at a range of frequencies and depths. By correlating the results with the ( $\gamma, \kappa$ ) model, we produce estimates of scattering, GS, and intrinsic attenuation within each layer of the model.

### Method

Similarly to Richards and Menke (1983) and Morozov (2011), we consider only normal-incidence reflectivity during propagation. This 1-D approximation focuses on scattering effects and appears to be reasonable for strongly layered and reflective structure within the Weyburn oilfield area. The medium is represented by a sequence of constant-impedance layers constructed directly from well-log data. For  $N$

layers (Figure 1), the amplitudes within layer  $N$  and 1 can be related by using scattering-matrix formulation:

$$\begin{pmatrix} u_+^N \\ u_-^N \end{pmatrix} = T_{N,1} \begin{pmatrix} u_+^1 \\ u_-^1 \end{pmatrix}, \quad (2)$$

where  $T_{N,1}$  is the transmission matrix and  $u$  denotes the scalar wave amplitude. Waves with subscripts '+' travel downward, and those with '-' travel upward. For  $N = 2$ ,  $T_{2,1}$  is the transmission matrix on a single boundary (Morozov, 2011):

$$T_{2,1} = \frac{1}{2Z_2} \begin{pmatrix} Z_1 + Z_2 & Z_1 - Z_2 \\ Z_1 - Z_2 & Z_1 + Z_2 \end{pmatrix}, \quad (3)$$

where  $Z_i$  denotes the impedances of the respective layers.

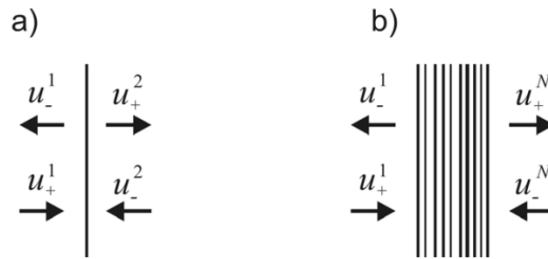


Figure 1: One-dimensional scattering model a) on a single boundary, b) on a sequence of  $N-1$  boundaries (from Morozov (2011)).

For  $N$  layers,  $T_{N,1}$  is a product of wave-mode transformations on all of the boundaries:

$$T_{N,1} = \prod_{i=2}^N T_{i,i-1} \begin{pmatrix} e^{i\Delta\varphi} & 0 \\ 0 & e^{-i\Delta\varphi} \end{pmatrix}, \quad (4)$$

where  $\Delta\varphi_i$  is the phase shift of the downward-traveling wave during its propagation within the layer  $i$ .

By recursively evaluating expressions (4), one can construct "logs" of transmission matrices  $T$ , upward- and downward- directed energy fluxes, etc., at any frequency ( $\omega$ ). We performed this calculation for frequencies from 0 to 200 Hz. The borehole logs used for this analysis contained P- and S-wave velocities and densities sampled at 10-cm intervals at depth from ~150 m to ~1500 m. Figure 2 shows the power spectrum of reflection coefficient to ~1390 m depth (top of reservoir caprock). The reflection coefficient generally continuously increases with frequency, which is related to the relatively slow roll-off of the spectrum of P-wave velocity (Figure 2, right). Figure 3 shows the modeled transmitted energy flux at the depths of 690, 918, 1162 and 1390 m.

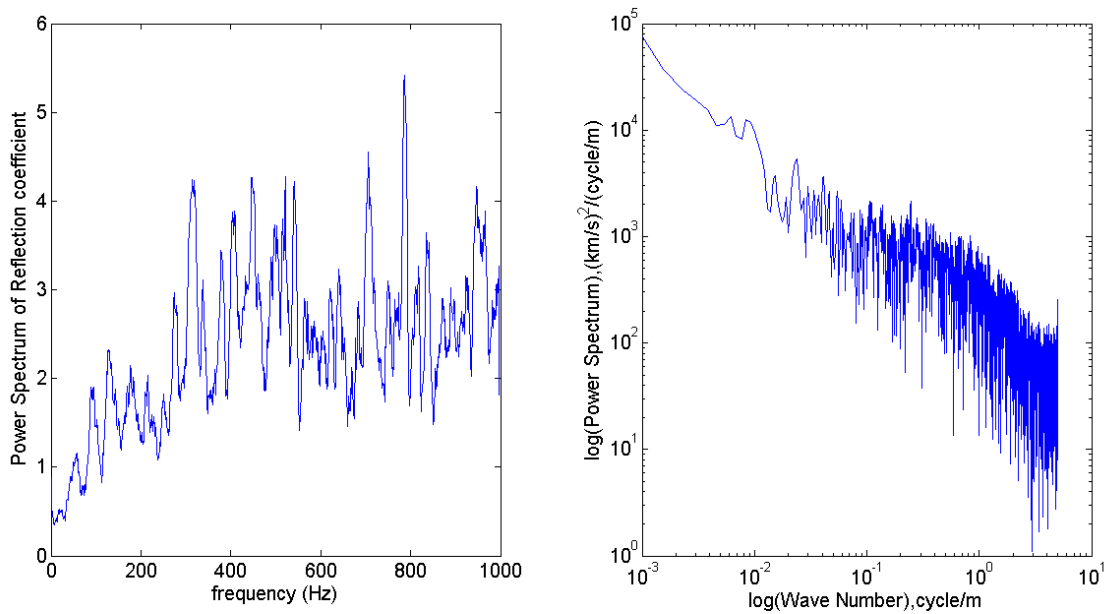


Figure 2: *Left*: Power spectrum of reflection coefficient versus frequency. *Right*: Power spectrum of  $V_P$  from the log versus wave number.

By considering a constant-time increment ( $\Delta\varphi = \text{const}$  in eq. (4)) approximation for the logs, O'Doherty and Anstey (1971) derived a simple relation between the power spectrum of the reflection-coefficient series,  $R(\omega)$ , and the amplitude spectrum of the pulse transmitted through it,  $T(\omega)$

$$T(\omega) = e^{-R(\omega)t}, \quad (5)$$

where  $t$  is the two-way travel time. These estimates of the transmitted energy flux are also shown by black curves in Figure 3.

Spectral-power plots in Figure 3 show generally exponential decreases of power with frequency, which can be described as  $T(\omega) \propto \exp[-2\chi(\omega)t]$ , with  $\chi(\omega)$  given by eq. (1), in which  $\gamma$  and  $\kappa$  are now responsible for scattering attenuation. Figure 4 shows the results of fitting equation (1) to the logarithms of the transmitted energy flux.

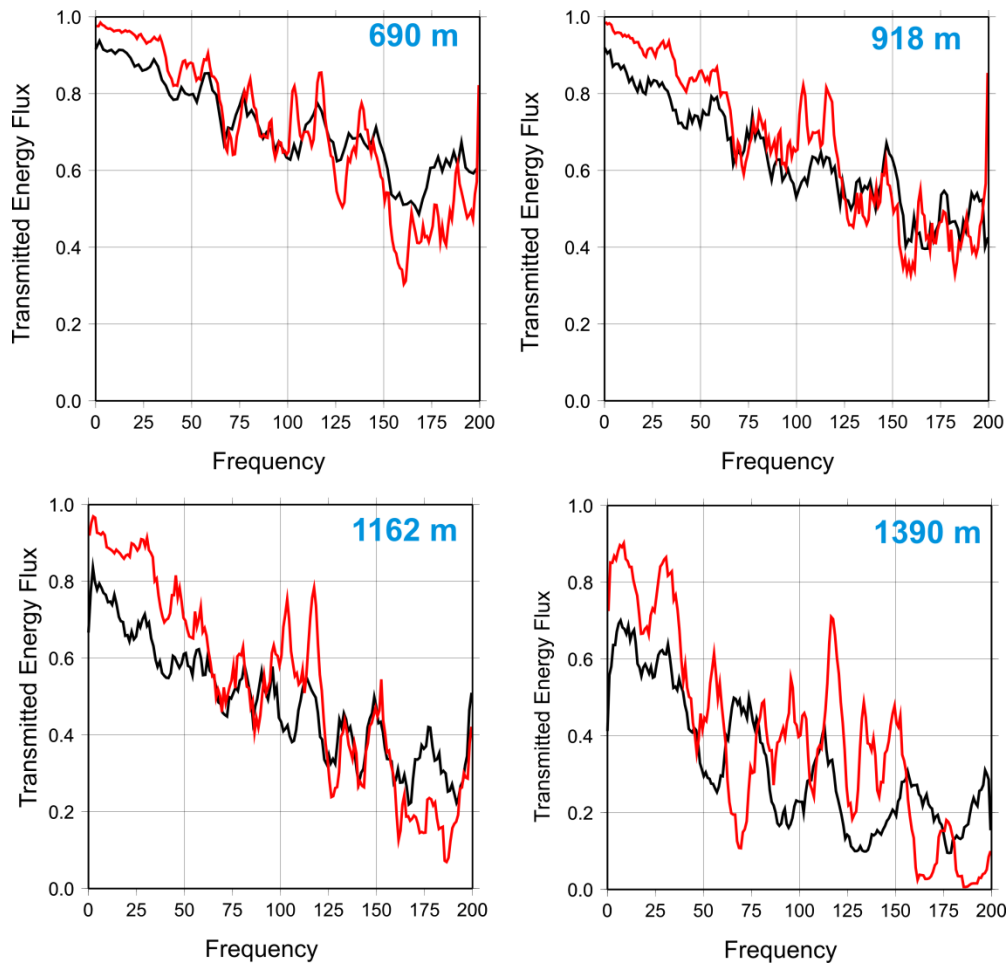


Figure 3: Power spectra of the transmitted energy flux from the beginning of the log (150 m) to different depths (blue labels), using eq. (4) (red) and eq. (5) (black).

## Results

Table 1 shows the “vertical” part of the attenuation model by Baharvand Ahmadi and Morozov (2012) with separate scattering GS, and internal-friction contributions. We also show estimates for the “effective quality factors”, defined by  $Q_e = \pi/\kappa$  (Morozov, 2008), for both scattering and internal friction. From these results, we can compare the relative effects of different attenuation factors in the data.

From

Table 1, it appears that at all depths, the GS has stronger effect than scattering:  $|\gamma_s| \ll |\gamma_{GS}|$ . This is likely due to our using a 1-D model for scattering. Also, within the upper layers (to ~690-m depth), the attenuation presented in the data is mostly intrinsic:  $|\kappa_{intrinsic}| \gg |\kappa_s|$ , whereas below this level, scattering  $\kappa_s$  is about 30% of  $\kappa_{intrinsic}$ . From ~918 to ~1162 m, scattering is ~3.6 times stronger than the internal friction. This increase in scattering can also be seen from log data, from an increase in reflectivity near the bottom of the VSP profile and especially around this interval.

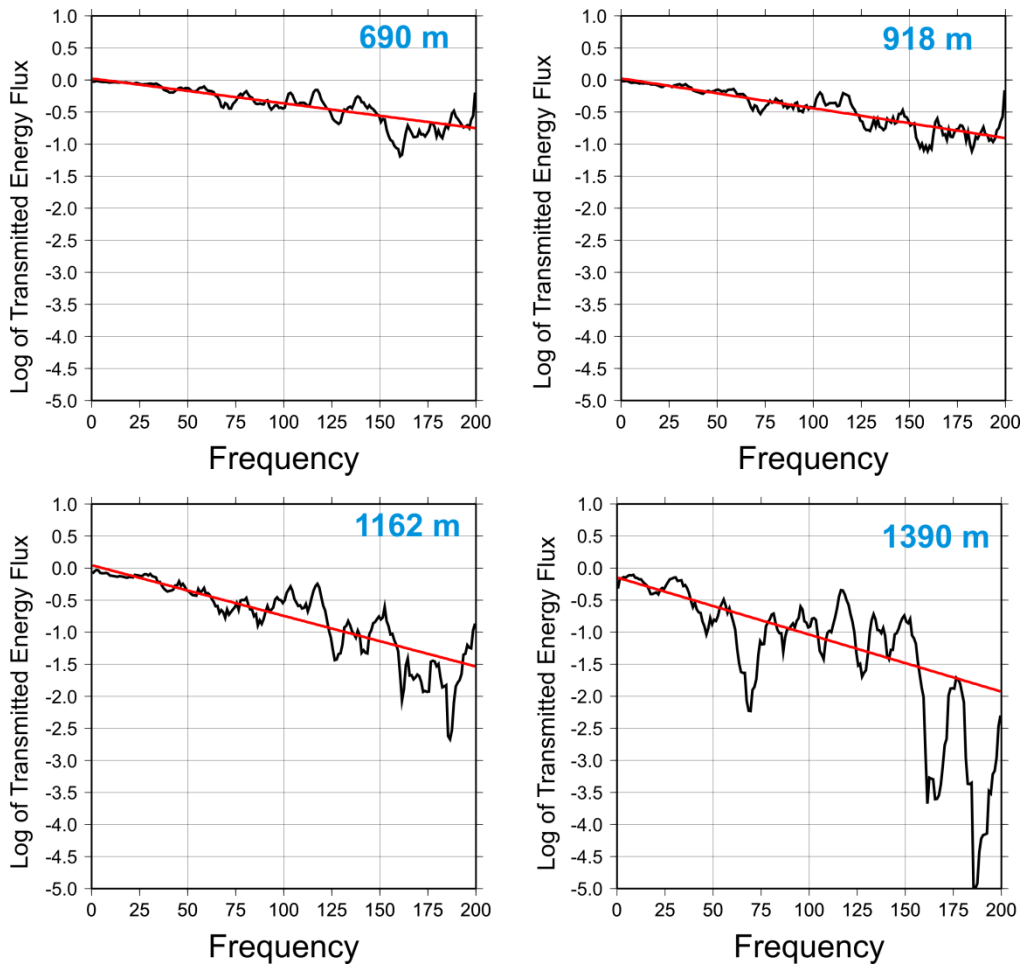


Figure 4: The results of fitting equation (1) to the logarithm of the transmitted energy flux from the top of the well log (~150 m) to selected depths (blue labels).

Table 1: Resulting separated geometric-spreading, scattering and intrinsic-attenuation model\*

Layer	Depth to bottom (m)	Velocity (m/s)	$\gamma_v$ (s <sup>-1</sup> )	$\kappa_v$	$\gamma_s$ (s <sup>-1</sup> )	$\kappa_s$	$Q_s = \pi / \kappa_s$	$\gamma_{GS}$ (s <sup>-1</sup> )	$\kappa_{intrinsic}$	$Q_{intrinsic} = \pi / \kappa_v$
1	295	2185	-2	0.12	0.09	0.005	628	-2.09	0.115	27
2	431	2230	-0.35	0.135	-0.15	0.010	314	-0.2	0.125	25
3	690	2330	1.23	0.0473	0.12	0.004	785	1.11	0.0433	72
4	918	2405	-0.24	0.0163	-0.03	0.004	785	-0.21	0.0123	255
5	1162	2970	3.92	0.0255	-0.07	0.02	157	3.99	0.0055	571
6	1390	3834	2.76	0.1437	1.02	0.03	104	1.74	0.1137	28

\*)  $\gamma_v$  and  $\kappa_v$  are the attenuation parameters in eq. (1) for vertical rays,  $\gamma_s$  and  $\kappa_s$  are the corresponding parameters for scattering,  $\gamma_{GS}$  is the estimated geometric spreading,  $\kappa_{intrinsic}$  is the internal friction,  $Q_s$  and  $Q_{intrinsic}$  are the effective quality factors for scattering and internal friction.

## Conclusions

A model of seismic scattering is derived from well logs in the VSP area in Weyburn oilfield. This model provides important observations about wave propagation with multiple reflections in finely layering media. The model allows separating the effects of scattering from those of geometrical spreading (GS) and intrinsic attenuation (internal friction). In Weyburn area, GS and internal friction effects dominate the decay of seismic amplitudes. Below ~690-m depths, scattering becomes important, and from ~930 to 1160 m, scattering dominates the frequency-dependent part of attenuation.

## Acknowledgements

This study was supported by IEA GHG Weyburn CO<sub>2</sub> Storage and Monitoring Project and by NSERC Discovery Grant RGPIN261610-03.

## References

- Baharvand Ahmadi, A., and I. Morozov, 2012, Anisotropic Frequency-Dependent Spreading of Seismic Waves from VSP Data Analysis: 2012 CSPG/CSEG/CWLS Convention.
- Dainty, A.M., 1981, A scattering model to explain seismic Q observations in the lithosphere between 1 and 30 Hz: *Geophysics, Res. Lett* **8**, 1126-1128.
- Frankel, A.D. and Wennerberg. L., 1987, Energy-flux model of seismic coda: Separation of scattering and intrinsic attenuation: *Bull. seism. Soc. Am.*, **77**, 1223-1251.
- Mayeda, K., Su, F. and Aki, K., 1991, Seismic albedo from the total seismic energy dependence on hypocentral distance in southern California: *Phys. Earth Planet. Inter.*, **67**, 104-114.
- Morozov, I. B., 2008, Geometric attenuation, frequency dependence of Q, and the absorption band problem: *Geophysical Journal International*, **175**, 239–252.
- Morozov, I. B., 2011, Mechanisms of geometric attenuation: *Annals of Geophysics*, **54**, 235–248, doi: 10.4401/ag-4780.
- O'Doherty, R. F., and Anstey, N. A., 1971, Reflections on amplitudes: *Geophysical Prospecting*, **19**, 430–458.
- Richards, P.G., and W.Menke., 1983, The apparent attenuation of a scattering medium, *Bull. Seism. Soc. Am.*, **75**, 1005-1021.
- Shearer, P. M., 1999, *Introduction to Seismology*: Cambridge University Press.